

FREE SURFACE FLOW IN VICINITY OF AN IMMERSSED CYLINDER

Nicoleta Octavia TĂNASE, Diana BROBOANĂ, Corneliu BĂLAN

“Politehnica” University of Bucharest, Hydraulic Department, Reorom Laboratory, Romania
E-mail: notanase@yahoo.com

The paper is concerned with experimental and numerical investigations of the flow around an immersed cylinder, in the presence of free surface. The main goal of the study is to establish a CFD procedure to compute the free surface geometry and the flow pattern in the neighborhood of the cylinder. The experiments are performed in a 2D channel, the flow rate and the fluid height upstream the body being controlled by a weir. The motion takes place in the transitory sub-critic regime with the characteristic Reynolds and Froude numbers in the ranges: $5000 < Re < 10000$, respectively $Fr < 1$. Qualitative direct visualizations of the flow and quantitative PIV measurements of the velocity distribution are obtained in the domain between the cylinder and the free surface. The computations have been performed with several turbulent models implemented in FLUENT code and the free surface geometry is calculated by the VOF model. The numerical results and visualizations are corroborated with the aim to investigate the interaction between the free surface and the wake developed downstream the separation points.

Key words: flow visualization, CFD, free surface, immersed cylinder, Reynolds number, Froude number.

1. INTRODUCTION

The flow around an immersed cylinder is a very actual "study case" for the free surface fluid mechanics, with numerous direct applications in hydrology, hydraulics and hydraulic turbines, marine platforms, inflatable dams, [3, 11, 14]. This particular motion, which is also of interest for fundamental research in fluid mechanics (in relation to hydraulic jumps, boundary layer theory, flow instabilities) is characterized by two non-dimensional parameters: the Reynolds number and the Froude number [16, 18]

$$Re = \frac{\rho V_0 D}{\eta}, \quad Fr = \frac{V_0}{\sqrt{gD}}, \quad (1)$$

where V_0 is the average velocity upstream of the cylinder, D is the diameter of cylinder, ρ is the density, η is the viscosity and g is the gravitational acceleration. As function of the parameters values, the free surface flow is classified as laminar or turbulent, in sub-critic or critical regimes.

One of the most important subject related to the hydrodynamics of free surface flows, which might be considered as a novel benchmark problem in fluid mechanics, is the solution of 2D channel flow around an immersed cylinder, respectively the computations of the free surface and the flow spectrum downstream the cylinder [5, 9].

Theoretical, numerical and experimental studies on the flow around a cylinder located in the vicinity of the free surface are at the beginning and the published literature in the domain is limited. All papers mentioned in the references are looking to this subject as a CFD application, in which the main target is to find the best numerical code which is able to reproduce the visualized flow field. The investigations are focused to the study of the downstream wake, the influence of the Froude number on the flow pattern, respectively the influence of the immersed depth, [6, 7, 10, 15, 16, 21] and the mechanism of the vorticity transfer from the free surface to the wake [18]. No special attention was given until now to the computation of the free surface geometry.

The main goal of the present study is to establish a CFD procedure to compute the free surface and the flow pattern in the neighborhood of the cylinder. The experiments are performed in a 2D open channel geometry, the flow rate and the fluid height upstream the body being controlled by a weir. The motion takes place in the transitory sub-critic flow regime with the characteristic Reynolds and Froude numbers in the ranges: $5000 < Re < 10000$, respectively $Fr < 1$. Qualitative direct visualizations of the flow and quantitative PIV measurements of the velocity distribution have been performed in the domain between the upper wall of the cylinder and the free surface. Numerical solutions for the flow are obtained with standard $k-\varepsilon$ and RNG $k-\varepsilon$ turbulent models and the free surface geometry is calculated by the Volume of Fluid (VOF) model available in FLUENT code.

The investigated flow regimes correspond to three immersed depths of the cylinder, but the numerical analysis is developed for one single case. The results of computations are compared with the experimentally free surface line and the wake pattern. The RNG $k-\varepsilon$ model is validated in the whole investigated domain, less for the free surface profile at the onset of the hydraulic jump. In that region, immediately downstream the minimum water depth, the flow regime is unsteady and the free surface discloses chaotic fluctuations.

The experimental set-up and the procedure of recording the trace of free surface are presented in the paragraph 2. The paragraph 3 is dedicated to the numerical simulations of the flow, where is shown the comparison between the computed profile of free surface and the experimental one. The results of the work are finally summarized and discussed in the last paragraph.

2. EXPERIMENTAL SET-UP AND FREE SURFACE PROFILE

The experiments are performed in a free surface transparent water channel of total length $L = 1232$ mm and a rectangular cross-section of maximum height $H_{\max} = 150$ mm and constant width $B = 15$ mm, [19, 20]. The cylinder with diameter $D = 50$ mm is located at the distance $L_1 = 303$ mm from the entrance section, which is connected to a constant level water supply tank. In the middle of the channel a weir is fixed (thickness $b_w = 6$ mm) which controls the transported flow rate and, in consequence, the free surface level, (Fig. 1). The total flow rate is divided around the cylinder, $Q = Q_1 + Q_2$, and no fluid leakage is noticed between the cylinder and the lateral walls of the channel.

The visualizations and measurements were performed at three constant entrance water levels H_0 , in the interval $92 < H_0 < 115$ mm. In all cases the height of the weir was kept constant at the value $h_w = 64$ mm (Fig. 1). The flow characteristics and the values of Reynolds and Froude numbers obtained from measurements are presented in Table 1.

Table 1

Flow characteristics and the values of Reynolds and Froude numbers (the numerical analyzed case is marked)

H_0 [mm]	h [mm]	Q [m ³ /s]	V_0 [m/s]	Re [-]	Fr [-]
92	7	0.1457	0.1	5000	0.143
105	20	0.2415	0.15	7500	0.214
115	30	0.3289	0.2	10000	0.285

The trace of the free surface line (FSL), considered as the intersection between the middle channel plane and the 3D free surface, was determined using series of high resolution images taken with a Sony SLT camera, at frequency of 12 frames/s. For the measurements of FSL profile, $y_0(x)$, was used as reference level the parallel line with the channel bottom corresponding to the centre of the cylinder (Fig. 2a).

The h – height represents the characteristic depth of the flow around an immersed cylinder [16, 18]; it is defined as the distance between the upper surface of the cylinder and the unperturbed free surface line, in our case being measured at the distance $x = 180$ mm upstream the centre of the cylinder (Fig. 1).

Experimentally, it is noticed that flow regime is always stationary upstream the cylinder. At few millimetres upstream of the impact point on the cylinder surface, the hydraulic jump starts to develop and the free surface discloses 3D-fluctuations (Fig. 2b), so the flow in this area is unsteady (characteristic which is maintained until the vicinity of the weir). Some periodicity of the flow was noticed, but fluctuations of free

surface disclose a chaotic profile, especially in region immediately downstream the cylinder. At small h – heights, these fluctuations are associated with Kelvin-Helmholtz instabilities developed in the fluid gap between the cylinder and free surface (Fig. 3a), phenomena which will be considered for our further studies.

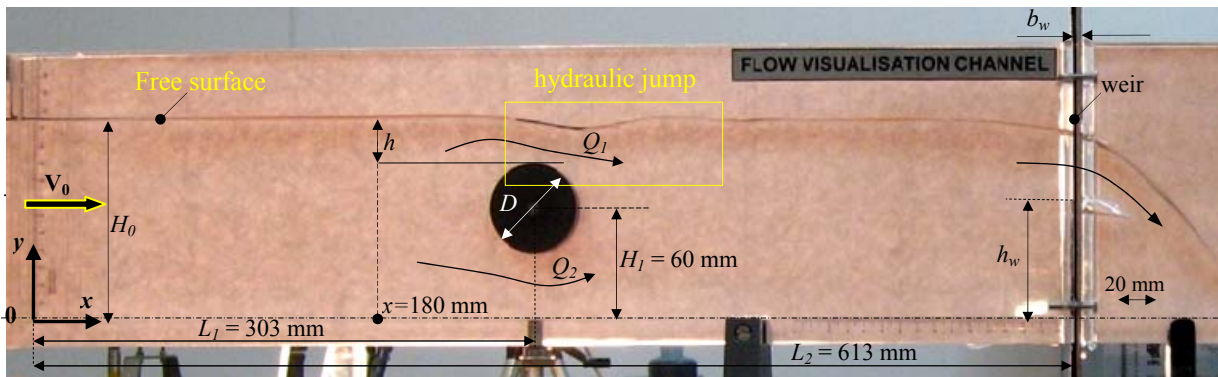


Fig. 1 – A sketch of the flow configuration and open channel geometry. The computational domain and boundary conditions are presented in Fig. 5. The domain of interest, where hydraulic jump takes place, is marked on the figure.

The focused planar surface of the camera is the middle plane of the channel, but the reflections of the front transparent channel wall are also recorded. The measurements of the FSL are affected by the capillarity and the fluctuation of the free surface curvature, therefore the experimental error is in the range of the capillary length, which corresponds to the value $h^* \approx 2.6$ mm (Fig. 2c). We expect this error to be relevant in the region corresponding to the onset of hydraulic jump and high fluctuations (Fig. 2b). Since the y_0 – distance is always taken in the picture at the lower captured trace of the free surface, the measured FSL profile is considered to be the minimum reached free surface level in the cross section.

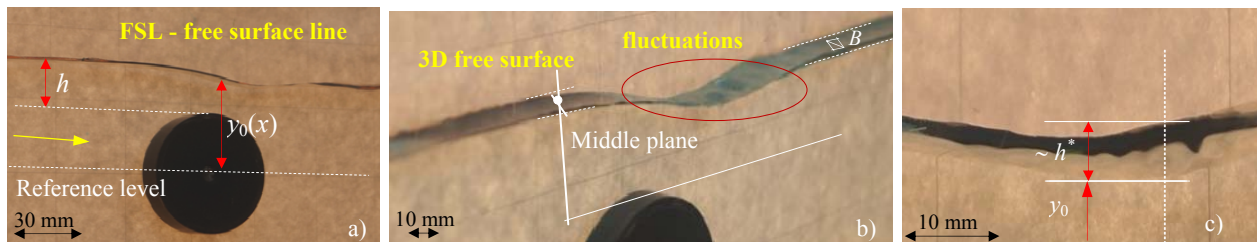


Fig. 2 – Visualization of free surface and the free surface line (FSL): a) FSL and the reference level, $y_0(x)$; b) 3D profile of the free surface; FSL line is obtained as the intersection of the real 3D free surface with the middle plane, which is the focused camera plane; c) detail with the FSL in the region of fluctuations and the effect of capillarity on the measurements.

The direct visualization of the streak lines, wake and vortical structures developed downstream the cylinder are obtained simultaneously with the free surface profile. The coloured tracers are introduced in the flow field through very thin needles located far upstream the cylinder or by injection of the dye from outside, directly into 36 holes distributed equally on the cylinder surface. The pictures show the location of separation (critical) points D_1 and D_2 (Fig. 3), for three different h – heights (details are given in [19]).

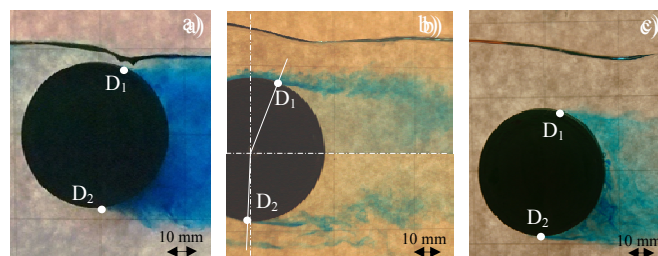


Fig. 3 – Direct visualizations of the free surface and the wake: a) $h = 7$ mm, b) $h = 20$ mm and c) $h = 30$ mm.

The measured profiles of free surface during the period of 1 s are shown in Fig. 4. The corrected standard deviation (CSD) and the mean values of the measured profile of FSL, which will be considered for comparison with numerical simulations, are marked in the plot.

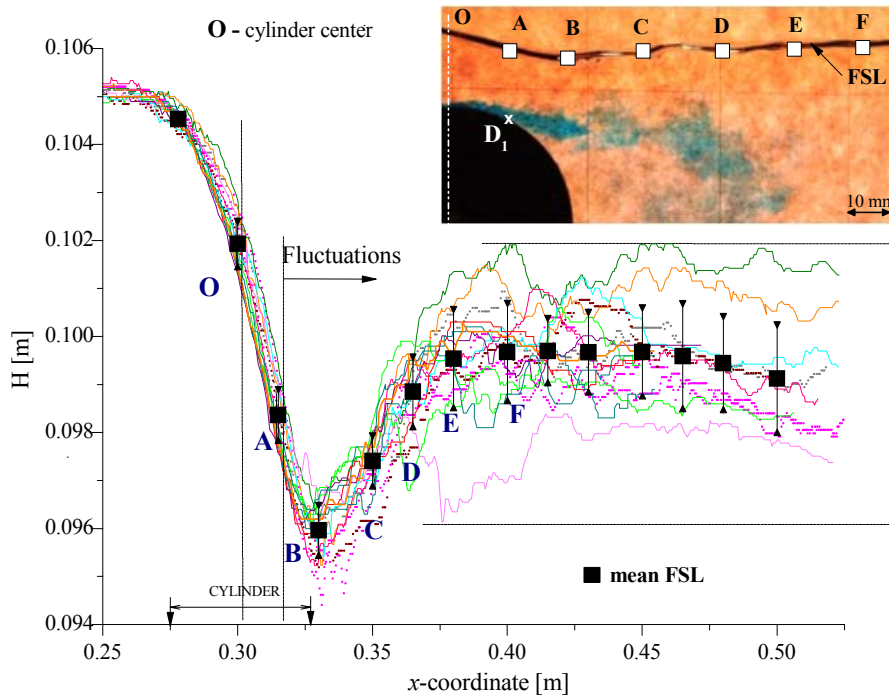


Fig. 4 – Instantaneously free surface lines recorded at 12 frames/s; the mean FSL and the corrected standard deviations are also represented. The fluctuations of free surface starts immediately after the separation point D_1 and are developing downstream the cylinder in a band of 4 mm width. Minimum of FSL corresponds to the end of cylinder.

3. NUMERICAL SIMULATIONS

The aim of the numerical study is to compute the free surface line (FSL) and to reproduce the flow spectrum around the cylinder, with the focus on the downstream wake. In particular, the main interest is to determine the flow kinematics in the gap between the cylinder and the free surface.

Numerical simulations are performed with the FLUENT code, which solves momentum and continuity (RANS) equations based on finite volume method [22],

$$\rho \left(\frac{\partial \tilde{\mathbf{v}}}{\partial t} + (\tilde{\mathbf{v}} \cdot \tilde{\nabla}) \tilde{\mathbf{v}} \right) = \rho \tilde{\mathbf{b}} - \text{grad} \tilde{p} + \text{div} \tilde{\mathbf{T}}_E, \quad (2)$$

$$\text{div} \tilde{\mathbf{v}} = 0.$$

In (2) $\tilde{\mathbf{v}}$ and \tilde{p} are the mean velocity and pressure; the mean extra-stress tensor $\tilde{\mathbf{T}}_E = 2(\eta_0 + \eta_t) \tilde{\mathbf{D}}$ includes the shear viscosity η_0 and the turbulent viscosity η_t , where $\tilde{\mathbf{D}}$ is the mean stretching. The k - ε models consider $\eta_t = \rho C_\mu k^2 / \varepsilon$, where C_μ is a constant ($C_\mu \cong 0.09$), k (the specific turbulent kinetic energy) and ε (the specific turbulent dissipation rate) being given by the corresponding transport equations.

The computations are performed on a 64 bit server Dual 2.33 GHz with 16 GB RAM memory, the computation time for each case being around 4 days, for a precision of 10^{-5} . Two turbulent models are considered in the present simulations: standard k - ε and the RNG (Re-Normalization Group) k - ε models (with standard wall functions) are run using steady and unsteady solvers. For the model discretization, the SIMPLE scheme was employed for pressure-velocity coupling, QUICK for the momentum and the transport equations.

The equations (2) are coupled with the Volume of Fluid (VOF) model available in FLUENT [1, 2, 4, 9, 17, 22]. In VOF procedure the computations are performed simultaneously in the whole domain for the two immiscible fluids (water and air in our case) and in each cell is calculated the volumetric fraction between the two phases. The flow separation water-air line is traced using the *modified HRIC* (High Resolution Interface Capturing) reconstruction procedure and implicit scheme. The reference computed FSL line is drawn through the cells which contain 50% of each phase [22]. The computational geometry is the 2D configuration of the channel (Fig. 1). The mesh contains 638.436 cells, 1.270.606 faces and 632.170 nodes; it is structured around the cylinder, the corresponding values of dimensionless wall distance y^+ are in the range of $0 < y^+ < 7$.

The initial distribution of the phases and the corresponding boundary conditions are shown in Fig. 5a: (i) inlet water ($x = 0$): the height $H_0 = 105$ mm kept constant imposing the linear pressure distribution $p = \rho gy$, $0 \leq y \leq H_0$; (ii) inlet – air, top-air and outlet: constant atmospheric pressure, $p = p_0$; (iii) adherence conditions on the weir and the lower wall: $\mathbf{v} = \mathbf{0}$. The final distribution of the phases and the free surface line (steady state) is shown in the detail (Fig. 5b).

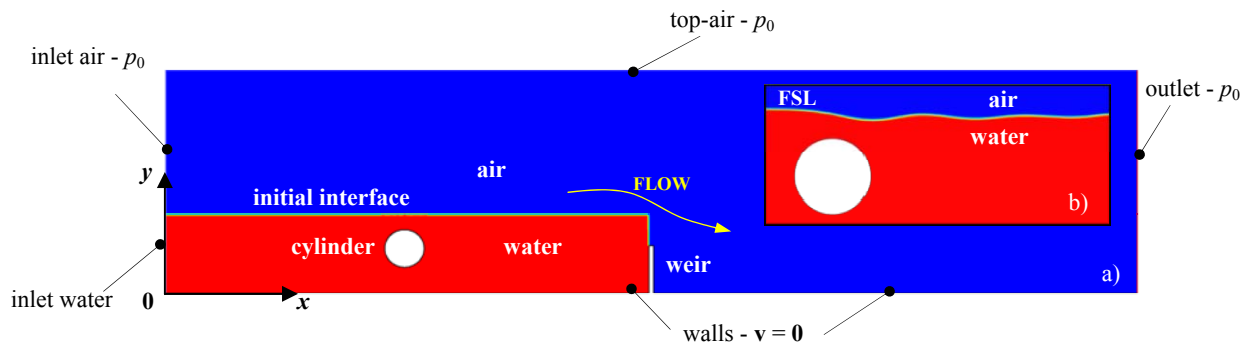


Fig. 5 – Numerical computational domain, a) initial phases configurations and the boundary conditions; b) detail with the final distribution of the phases and the free surface line (FSL).

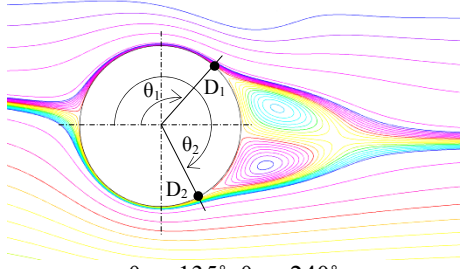
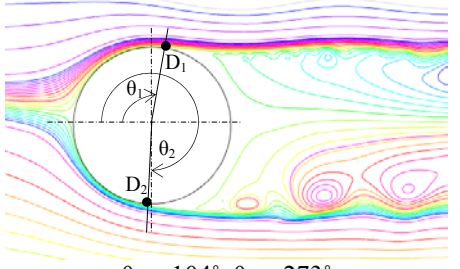
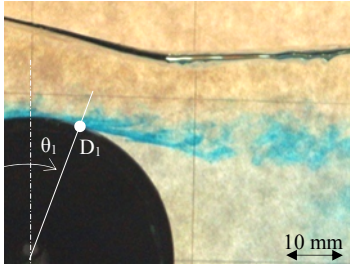
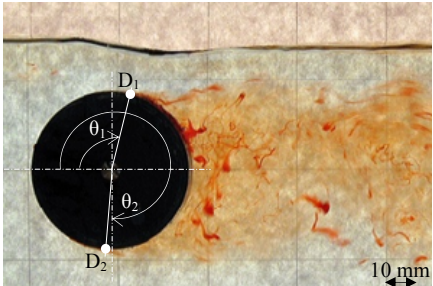
In Table 2 are presented the results for the computed steady flow spectrums, in comparison with the direct visualizations. The locations of the separation points on the cylinder are well reproduced by the RNG $k-\varepsilon$ model. The computed steady and unsteady free surface lines are compared with the experimental FSL in Fig. 6. One can be noticed that experimental free surface line upstream of the cylinder is perfectly reproduced numerically, but the oscillations downstream the cylinder are captured only by the RNG $k-\varepsilon$ model. The fitting of free surface in the domain of hydraulic jump is considered fair. The maximum difference between the experimental and numerical free surface is of 3.2 mm, recorded at the end of the immersed cylinder (Fig. 6b), value which represent an absolute error of 3% from the average height of the water in that point of the channel. The analysis of the numerical results (free surface profile, location of separation points, wake structure) in comparison with experiments concludes that RNG $k-\varepsilon$ turbulence model is more indicated to simulate the flow under investigation.

Solutions with the unsteady solver have been also obtained for the RNG $k-\varepsilon$ turbulence model, using the time step of 0.001 s, for a precision of 10^{-5} . The numerical results are shown in Fig. 6 in comparison with experiments and steady solution. Based on the analysis of the results displayed in Fig. 7, and also taking into account the very long time needed for computation of the unsteady solutions, one can conclude that steady solver offers a fair representation of the average time free surface configuration. There are several differences between the numerical results and the experimental FSL, especially in the region between the separation point D_1 and the end of cylinder, mainly due to the high curvature and fluctuations of the free surface. The capillarity phenomenon and the photographic image deformation can also induce some errors in measurements. Actually, the visualized free surface is a band (Fig. 2a), and the measured values correspond to the lowest level of this band (Fig. 7a), the numerical free surface being in almost all cases at higher level than experiments. Comparisons between numerical and experimental results were made also quantitative using the PIV system. For the PIV measurements was used a CMOS Nano Sense MKII camera, with a

maximum acquisition rate of 5 kHz at a resolution of 512×512 pixels. The light source was an infrared laser Nanopower with a power of 4 W and a wavelength of 795 nm. The seed particles are glass spheres coated with a silver layer. The measured velocity fields between the cylinder and the free surface confirm the numerical results and validate also quantitatively the RNG $k-\varepsilon$ turbulence model for this type of flows [2, 8, 12, 13]. The results of the PIV measurements are presented in Fig. 7.

Table 2

Comparison between computed and visualized flow spectrums for the reference case (Table 1). The steady solutions obtained with RNG $k-\varepsilon$ model offer a better representation of the real flow than the standard $k-\varepsilon$ model

Models	standard $k-\varepsilon$	RNG $k-\varepsilon$
Properties of the model	The model is proper for fully developed turbulent flows (known as a high-Reynolds- number model).	The RNG theory provides an analytically-derived differential formula for effective viscosity that accounts for low-Reynolds-number effects. The model is better suited for turbulent flows in vicinity of stagnation and separation points.
Numerics	 $\theta_1 = 135^\circ, \theta_2 = 240^\circ$	 $\theta_1 = 104^\circ, \theta_2 = 273^\circ$
Experimental (direct visualization)	 Detail, $\theta_1 = 110^\circ$	 The wake downstream the cylinder, $\theta_2 = 273^\circ$

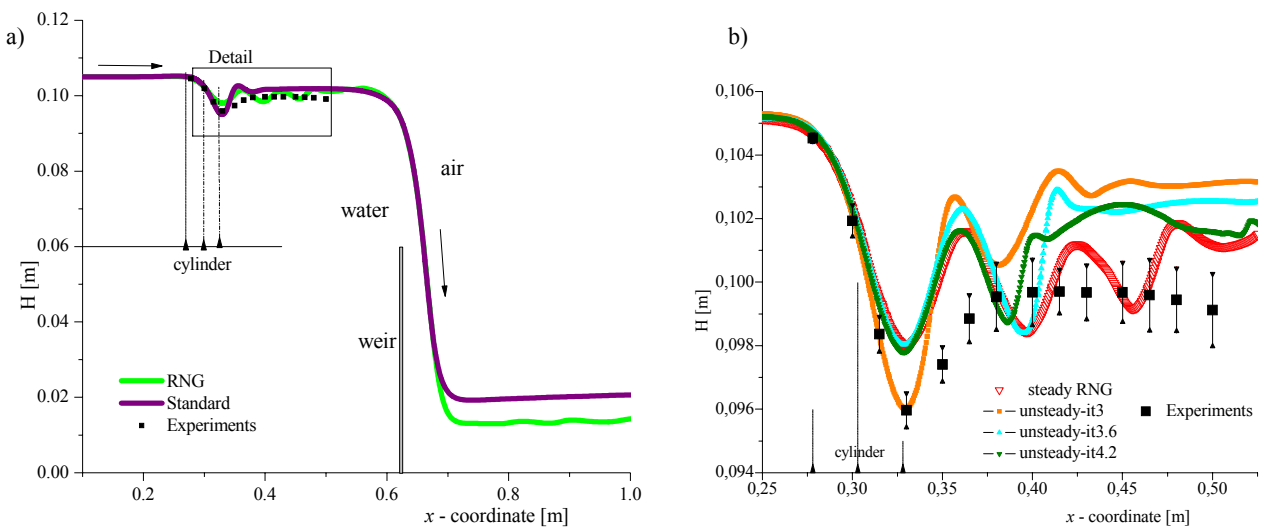


Fig. 6 – a) Comparison of the experimental free surface line with the numerical steady solutions for the two $k-\varepsilon$ models; b) steady and unsteady numerical solutions (corresponding at 3 s, 3.6 s and 4.2 s) and experimental data are shown (Fig. 4).

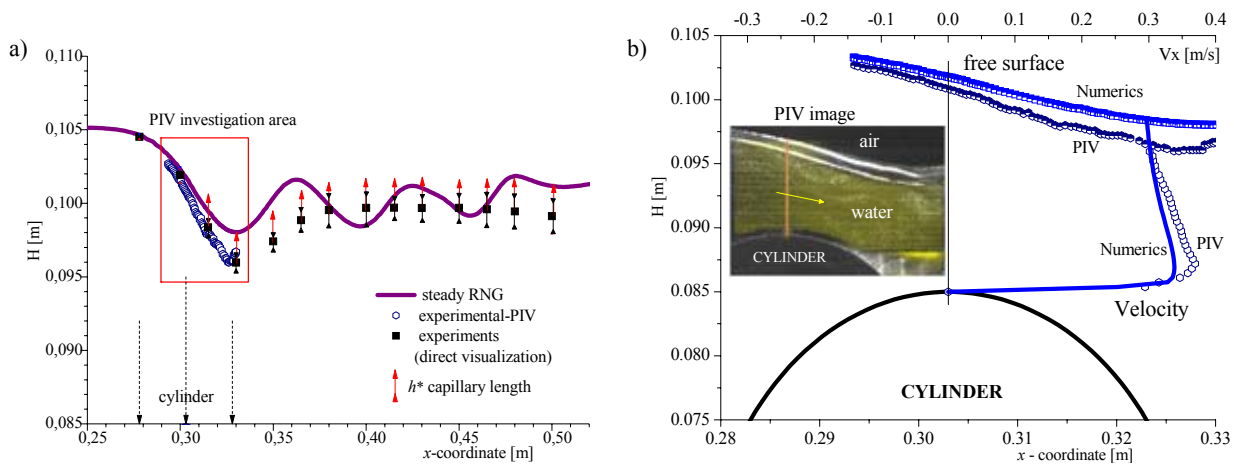


Fig. 7 – Comparison between computations and experimental investigations: a) free surface line (CSD bar and the capillary length are shown); b) velocity distribution v_x corresponding to the center of the immersed cylinder.

5. CONCLUSIONS

The paper was dedicated to the experimental and numerical investigations of the flow around an immersed cylinder, in the presence of free surface. The study established a CFD procedure to compute the free surface geometry and the flow pattern in the neighborhood of the cylinder for “weak turbulent flows” in sub-critical regimes, i.e. the characteristic Reynolds and Froude numbers are within the ranges: $5000 < Re < 10000$, respectively $Fr < 1$. The numerical procedure based on the RNG $k-\varepsilon$ turbulence model and steady solver was validated for 2D configuration by the experiments performed in a free surface 2D water channel. The free surface line was experimentally obtained using both streak lines direct visualizations and quantitative PIV velocity measurement in the gap between the free surface and the cylinder.

The numerical trace of the free surface fit very well the experiments, except of the region downstream the cylinder where the numerical solution reproduces only qualitatively the fluctuations observed in the real flow. However, the proposed CFD procedure gives a fair representation of the free surface geometry in vicinity of the cylinder.

The present result is very promising and offers possibilities to investigate in more details the local hydrodynamics around the immersed bodies, especially in relation to Kelvin-Helmholtz instabilities developed in the region between the free surface and the wake downstream the body. The further study will be focused to the investigation of possible correlation between the frequency fluctuations of the free surface and the vortex detachment frequency from the cylinder, at low immersed depths of the cylinder where the influence of surface tension is expected to be observed.

ACKNOWLEDGMENTS

The authors acknowledge the financial support received from the grant UEFISCDI project PN-II-ID-PCE-2012-4-0245/2013. Nicoleta Octavia Tanase’s work has been funded by the Sectoral Operational Programme Human Resources Development 2007-2013 of the Ministry of European Funds through the Financial Agreement POSDRU/159/1.5/S/132395. The assistance and support of the Professor Iilca Nastase (UTCM) in obtaining the PIV measurements is also acknowledged.

REFERENCES

1. BAKKER A., *Applied computational fluid dynamics – Turbulence models*, <http://www.bakker.org>, 2002-2006.
2. BROBOANĂ D., MUNTEAN T., BĂLAN C., *Experimental and numerical studies of weakly elastic viscous fluids in a Hele-Shaw geometry*, Proc. of the Romanian Academy, Series A, Mathematics, Physics, Technical Science, **8**, 3, pp. 219–233, 2007.
3. CHAMORRO L.P., HILL C., MORTON S., ARNDT R. E. A., ELLIS C., SOTIROPOULOS F., *On the interaction between a turbulent open channel flow and an axial-flow turbine*, J. Fluid Mech., **716**, pp. 658–670, 2013.

4. DĂNĂILĂ S., BERBENTE C., *Metode numerice in dinamica fluidelor*, Edit. Academiei, București, 2003.
5. DONG S., KARNIADAKIS G.E., *DNS of flow past a stationary and oscillating cylinder at $Re = 10\,000$* , J. Fluids and Structures, **20**, pp. 519–531, 2005.
6. DONG S., KARNIADAKIS G. E., EKMEKCI A., ROCKWELL D., *A combined direct numerical simulation –particle image velocimetry study of the turbulent near wake*, J. Fluid Mech., **569**, pp. 185–207, 2006.
7. HONZEJK V., FRAŇA K., *A turbulent flow past a cylinder*, J. Applied Science in the Thermodynamics and Fluid Mechanics, **2**, pp. 1–6, 2008.
8. HOYT J. W., SELLIN R. H. J., *A comparison of tracer and PIV results in visualizing water flow around a cylinder close to the free surface*, Exp. Fluids, **28**, pp. 261–265, 2000.
9. LAUNDER B. E., SPALDING D. B., *Mathematical models of turbulence*, Academic Press, London, 1972.
10. LEE S.J., DAICHIN, *Flow past a circular cylinder over a free surface: Interaction between the near wake and the free surface deformation*, J. Fluids and Structures, **19**, pp. 1049–1059, 2004.
11. LIN M.Y., HUANG L.H., *Free-surface flow past a submerged cylinder*, J. Hydrodynamics, **22**, 5, pp. 209–214, 2010.
12. MYERS L.E., BAHAJ A.S., *Experimental analysis of the flow field around horizontal axis tidal turbines by use of scale mesh disk rotor simulator*, Ocean Engineering, **37**, pp. 218–227, 2010.
13. NĂSTASE I., MESLEM A., BOWMANS T., *Vortical structures analysis in jet flows using a classical 2D-PIV system and time resolved visualization image processing*, J. Flow Visualization and Image Processing, **15**, 9, pp. 275–300, 2008.
14. ONG M.C., *Applications of a standard high Reynolds number $k-\epsilon$ model and a stochastic scour prediction model for marine structures*, PhD. Thesis, Norwegian University of Science and Technology, 2009.
15. OSHKAI P., ROCKWELL D., *Free surface wave interaction with a horizontal cylinder*, Journal of Fluids and Structures, **13**, pp. 935–954, 1999.
16. REICHL P.J., HOURIGAN K., THOMPSON M. C., *Flow past a cylinder close to a free surface*, J. Fluid Mech., **533**, pp. 269–296, 2005.
17. SCHLICHTING H., GERSTEN K., *Boundary layer theory*, Springer, Berlin, 2000.
18. SHERIDAN J., LIN, D. ROCKWELL, *Flow past a cylinder close to a free surface*, J. Fluid Mech., **330**, pp. 1–30, 1997.
19. TĂNASE, N. O., *Modelarea curgerilor tranzitorii în jurul corpurilor aflate în vecinătatea suprafeței libere în regimul subcritic*, Ph.D. Thesis, Power Engineering Faculty, “Politehnica” University of Bucharest, Romania, 2013.
20. TĂNASE N. O., BROBOANĂ D., BĂLAN C., *Flow around an immersed cylinder in the presence of free surface*, Scientific Bulletin, Series D, UPB, **76**, 2, pp. 259–266, 2014.
21. WU M-H., WEN C-Y., YEN R-H., WENG M-C., WANG A-B., *Experimental and numerical study of the separation angle for flow around a circular cylinder at low Reynolds number*, J. Fluid Mech., **515**, pp. 233–260, 2004.
22. *** *Fluent 6.3 User’s Manual*, Fluent Inc., 2008.

Received August 8, 2014